Superconductivity in the Hubbard model with pair hopping

Stanisław Robaszkiewicz*
Department of Physics, Adam Mickiewicz University, ul. Umultowska 85, 61-614 Poznań, Poland

Bogdan R. Bułka†
Institute of Molecular Physics, Polish Academy of Sciences, ul. Smoluchowskiego 17, 60-179 Poznań, Poland
(Received 29 May 1998; revised manuscript received 4 September 1998)

The phase diagrams and superconducting properties of the extended Hubbard model with pair hopping interaction, i.e., the Penson-Kolb-Hubbard model are studied. The analysis of the model is performed for d-dimensional hypercubic lattices, including $d=1$ and $d=\infty$, by means of the (broken symmetry) Hartree-Fock approximations and, for $d=\infty$, by the slave-boson mean-field method. For $d=1$, at half filling the phase diagram is shown to consist of nine different phases including two superconducting states with center-of-mass momentum $q=0$ and $q=Q$ (η pairing), site and bond-located antiferromagnetic and charge-density wave states as well as three mixed phases with coexisting site and bond orderings. The stability range of the bond-type orderings shrinks with increasing lattice dimensionality d and for $d=\infty$ the corresponding diagram consists of four phases only, involving exclusively site-located orderings. Comparing the pair hopping model with the attractive Hubbard model we found in both cases gradual evolution from the BCS-like limit to the tightly bound pairs regime and a monotonic increase of the gap in the excitation spectrum with increasing coupling. However, the dynamics of electron pairs in both models is qualitatively different, which results in different dependences of condensation energies and critical temperatures on interaction parameters as well as in different electrodynamic properties, especially in a strong coupling regime. [S0163-1829(99)01909-8]

I. INTRODUCTION

The purpose of the present work is the analysis of phase diagrams, electronic orderings and superconducting properties of the extended Hubbard model with pair hopping interaction, i.e., the so-called Penson-Kolb-Hubbard (PKH) model

$$H=-t\sum_{i,j,\sigma}{}' \; c_{i\sigma}^{\dagger}c_{j\sigma}+U\sum_{i} \; n_{i\uparrow}n_{i\downarrow}$$

$$-J\sum_{i,j}{}' \; c_{i\uparrow}^{\dagger}c_{i\downarrow}^{\dagger}c_{j\downarrow}c_{j\uparrow}-\mu\sum_{i,\sigma} \; n_{i\sigma}, \qquad (1)$$

where the prime over the sum means restriction to nearest neighbor (nn) sites, t denotes the single electron hopping integral, U is the onsite density-density interaction, J is the pair hopping (intersite charge exchange) interaction, and μ is the chemical potential. In the absence of the U term the Hamiltonian (1) reduces to the Penson-Kolb (PK) model.[1]

We will treat the parameters t, U, J as the effective (phenomenological) ones, assuming that they include all the possible contributions and renormalizations such as those coming from the strong electron-phonon couplings or from the coupling between electrons and other electronic subsystems in solid or chemical complexes[2] (such that the values of U and J can be effectively either positive or negative). It is notable that formally J is one of the off-diagonal terms of the Coulomb interaction $-J=(ii|e^2/r|jj)$,[3] describing a part of the so-called bond-charge interaction, and the sign of the *Coulomb-driven* charge exchange is typically negative (repulsive, $J<0$). However, the effective attractive interaction of this form ($J>0$) is also possible[4–6] and in particular it can originate from the coupling of electrons with intersite (intermolecular) vibrations via modulation of the hopping integral,[4] or from the on-site hybridization term in a generalized periodic Anderson model.[5,6]

The PKH model is one of the conceptually simplest phenomenological models for studying correlations and for description of superconductivity of the narrow band systems with short-range, almost unretarded pairing. It includes a nonlocal pairing mechanism (the pair hopping term J) that is distinct from the on-site interaction in the attractive Hubbard model and that is the driving force of pair formation and also of their condensation. Thus, the superconducting properties and the evolution from the Cooper pair regime to the strong coupling local pair regime can be essentially different in these two models.

While most of the basic properties of the attractive Hubbard model seems to be at present well understood after several years of intense studies, the PKH model has been investigated only in a few particular limits.[1,7–15] The main efforts concerned the ground state phase diagram of the half-filled one dimensional PKH (Refs. 8, 9, 15) and PK (Refs. 7, 10, 12, 13) models. In the case of the PKH model these problems were studied by both, momentum-space renormalization-group (MSRG) and the finite-size (exact diagonalization of finite-size cells) methods (for $U,J>0$),[8] by the real space renormalization-group (RSRG) (for $U>0$),[11] by the continuum-limit field theory (CFT) approach[15] (for $U>0$), and within the Green's function formalism in the mean-field approximation.[9] However, in all these studies, except Ref. 15, the possibility for the bond-located orderings was not considered and the exact form of the phase diagram in the whole range of parameters $-\infty<U/t,J/t<\infty$ has not been established up to now. The properties of the PKH model for

 ©1999 The American Physical Society

higher-dimensional lattices ($1<d\leqslant\infty$) and arbitrary electron concentration ($0<n<2$) have not been studied yet, except for the limiting case of zero bandwidth.[16] The latter limit was analyzed by the variational approach, in which the U term is treated exactly and the intersite J term—within the mean-field approximation[16] (such an approach yields exact results for $d=\infty$).

In the paper we will study the PKH model for the case of d-dimensional hypercubic lattices ($1\leqslant d\leqslant\infty$) and arbitrary, positive, and negative U and J. In the analysis we will apply a broken symmetry Hartree-Fock approximation (HFA) (Sec. II) supplemented for $d=\infty$ by the slave boson mean-field approach (SBMFA) (Sec. III). In the case of the Hubbard model and its various extensions[2] the former approach is known to give credible results at $T=0$ for any U as far as the energy of the ground state and energy gap in the ordered states is concerned. It usually provides qualitatively correct ground state phase diagrams for arbitrary dimensions if all the proper broken symmetry phases are included into the analysis. Moreover, for the electronic models with intersite interactions only, the HFA becomes an exact theory in the limit of infinite dimension ($d=\infty$). At $T>0$ the HFA is much less reliable, especially for low dimensional systems and the limits of strong coupling, as it neglects short-range correlations and the effects of collective excitations. An obvious weakness of the HFA (both at $T=0$ and $T>0$) is inadequate description of the normal (nonordered) phase. This failure is a consequence of the fact that the HFA greatly overestimates the energy of the phases without long-range order. Going beyond the HFA we will use the SBMFA. The slave-boson method is in principle not restricted to weak or strong coupling and it is an improvement over the former treatment since it takes into account local correlations.[17] We will apply the SBMFA only for $d=\infty$, where the intersite coupling J can be treated adequately. For finite dimension ($d<\infty$) the SBMFA treatment of intersite interactions is technically involved and to our knowledge it has not been analyzed consistently so far.

II. GENERAL FORMULATION AND THE HARTREE-FOCK ANALYSIS

In the system considered several types of superconducting, magnetic, and charge orderings can develop. In the following we will study the case of alternating (hypercubic) lattices with nearest-neighbor single electron hopping t and pair hopping J, and restrict our considerations to the one- and two-sublattice orderings,[18] described by the following order parameters. The superconducting with s-type (S) and the η-type (η) pairing:

$$x_S=(1/N)\Sigma_i\langle c_{i\downarrow}c_{i\uparrow}\rangle=(1/N)\Sigma_k\langle c_{-k\downarrow}c_{k\uparrow}\rangle,$$

$$x_\eta=(1/N)\Sigma_i e^{i\mathbf{QR}_i}\langle c_{i\downarrow}c_{i\uparrow}\rangle=(1/N)\Sigma_k\langle c_{-k+Q\downarrow}c_{k\uparrow}\rangle.$$

The antiferromagnetic (AF) with the staggered magnetization located on sites (sAF) or on bonds between sites (bAF):

$$x_{\mathrm{sAF}}=(1/2N)\Sigma_{i,\sigma}\sigma e^{i\mathbf{QR}_i}\langle c_{i\sigma}^\dagger c_{i\sigma}\rangle,$$

$$x_{\mathrm{bAF}}=(1/2N)\Sigma'_{i,j>i,\sigma}\sigma e^{i\mathbf{QR}_i}\langle c_{i\sigma}^\dagger c_{j\sigma}\rangle$$
$$=(1/4N)\Sigma_{k,\sigma}\sigma\eta_k\langle c_{k\sigma}^\dagger c_{k+Q\sigma}\rangle,$$

the charge density wave (CDW) with the on-site (sCDW) or the bond zigzag (bCDW) modulation of charges: $x_{\mathrm{sCDW}}=(1/2N)\Sigma_{i,\sigma}e^{i\mathbf{QR}_i}\langle c_{i\sigma}^\dagger c_{i\sigma}\rangle$, $x_{\mathrm{bCDW}}=(1/2N)\Sigma'_{i,j>i,\sigma}e^{i\mathbf{QR}_i}\times\langle c_{i\sigma}^\dagger c_{j\sigma}\rangle=(1/4N)\Sigma_{k,\sigma}\eta_k\langle c_{k\sigma}^\dagger c_{k+Q\sigma}\rangle$, where $\eta_k=i\Sigma_a\times\sin(ka)$ and $Q=(\pi/a,\pi/a,\ldots)$. We assume that the sites are ordered in an ascending way along the crystallographic axis and for the case of the bond zigzag parameters the sum is restricted to the nearest neighbor sites j, which followed the ith site. The number of electrons per lattice site is given by $n=(1/N)\Sigma_{i,\sigma}\langle c_{i\sigma}^\dagger c_{i\sigma}\rangle$. In the case of the AF phase we quoted above only sAF_z and bAF_z orderings, corresponding to a z-component magnetization located on sites and bonds, respectively, and we omitted $\mathrm{s(b)AF}_x$, $\mathrm{s(b)AF}_y$. Due to the SU(2) spin symmetry of the PKH model the latter orderings are strictly degenerated with $\mathrm{s(b)AF}_z$.

Within the framework of the broken-symmetry Hartree-Fock approach the mean-field Hamiltonian in the momentum space k, including all types of orderings is given by

$$H_{HF}=\sum_{k,\sigma}\left(\epsilon_k-\mu+\frac{U}{2}n\right)c_{k\sigma}^\dagger c_{k\sigma}+(U-zJ)$$
$$\times\sum_k\ (x_S c_{k\uparrow}^\dagger c_{-k\downarrow}^\dagger+\mathrm{H.c.})+(U+zJ)$$
$$\times\sum_k\ (x_\eta c_{k\uparrow}^\dagger c_{-k+Q\downarrow}^\dagger+\mathrm{H.c.})-Ux_{\mathrm{sAF}}$$
$$\times\sum_{k,\sigma}\ \sigma c_{k\sigma}^\dagger c_{k+Q\sigma}+\frac{2J}{z}x_{\mathrm{bAF}}$$
$$\times\sum_{k,\sigma}\ \sigma\eta_k c_{k\sigma}^\dagger c_{k+Q\sigma}+Ux_{\mathrm{sCDW}}$$
$$\times\sum_{k,\sigma}\ c_{k\sigma}^\dagger c_{k+Q\sigma}-\frac{2J}{z}x_{\mathrm{bCDW}}\sum_{k,\sigma}\ \eta_k c_{k\sigma}^\dagger c_{k+Q\sigma},\quad(2)$$

where $\epsilon_k=-\tilde{t}\gamma_k$, $\tilde{t}=t+2pJ/z$, z is the number of nearest neighbor sites (for the hypercubic lattice of d dimension: $z=2d$), and p denotes the Fock term $p=(1/4N)\Sigma'_{i,j,\sigma}\langle c_{i\sigma}^\dagger c_{j\sigma}\rangle=(1/4N)\Sigma_{k,\sigma}\gamma_k\langle c_{k\sigma}^\dagger c_{k\sigma}\rangle$, with $\gamma_k=\Sigma_a\cos(ka)$.

The eigensolutions of the Hamiltonian (2) and the corresponding free energy

$$F=-\frac{1}{\beta}\ln[\mathrm{Tr}\{\exp(-\beta H_{\mathrm{HF}})\}]+\langle H-H_{\mathrm{HF}}\rangle_{\mathrm{HF}}+\mu N_e,\quad(3)$$

where $\beta=1/k_BT$ and N_e denotes the number of electrons in the system, can be determined by the standard methods[19] with either the Green's function or the equation of motion approach. If the solutions corresponding to the pure phases (i.e., the phases with only one type of order) are analyzed, the free energy (3) may be expressed in terms of the eigenvalues of H_{HF} in the form

TABLE I. Phases considered and the corresponding order parameters.

Type of phase	Order parameters
S	$x_S \neq 0$
η	$x_\eta \neq 0$
sAF	$x_{\mathrm{sAF}} \neq 0$
bAF	$x_{\mathrm{bAF}} \neq 0$
s+bAF	$x_{\mathrm{sAF}} \neq 0, x_{\mathrm{bAF}} \neq 0$
sCDW	$x_{\mathrm{sCDW}} \neq 0$
bCDW	$x_{\mathrm{bCDW}} \neq 0$
s+bCDW	$x_{\mathrm{sCDW}} \neq 0, x_{\mathrm{bCDW}} \neq 0$
bAF+sCDW	$x_{\mathrm{bAF}} \neq 0, x_{\mathrm{sCDW}} \neq 0$
sAF+bCDW	$x_{\mathrm{sAF}} \neq 0, x_{\mathrm{bCDW}} \neq 0$
S+sCDW	$x_S \neq 0, x_{\mathrm{sCDW}} \neq 0$
S+bCDW	$x_S \neq 0, x_{\mathrm{bCDW}} \neq 0$
η+sCDW	$x_\eta \neq 0, x_{\mathrm{sCDW}} \neq 0$
η+bAF	$x_\eta \neq 0, x_{\mathrm{bAF}} \neq 0$
η+sAF+bAF	$x_\eta \neq 0, x_{\mathrm{sAF}} \neq 0, x_{\mathrm{bAF}} \neq 0$

$$\frac{F}{N} = \bar{\mu}(n-1) + \frac{U}{4}n^2 + \frac{4}{z}Jp^2 + A_\alpha |x_\alpha|^2 - \frac{1}{\beta N}\sum_{k,r} \ln\left[2\cosh\left(\frac{\beta E^r_{\alpha k}}{2}\right)\right], \tag{4}$$

where $r=\pm$, $\bar{\mu}=\mu - Un/2$, V_α is an effective coupling strength for the α phase, which is $V_S=-U+zJ$, $V_\eta=-U-zJ$, $V_{\mathrm{sAF}}=U$, $V_{\mathrm{bAF}}=-2J/z$, $V_{\mathrm{sCDW}}=-U$ and $V_{\mathrm{bCDW}}=2J/z$, $A_\alpha=V_\alpha$ for $\alpha=S$, η, sAF, sCDW and $A_\alpha=2V_\alpha$ for $\alpha=$ bAF, bCDW. The electronic spectrum is $E^{\pm}_{Sk}=\pm\sqrt{(\epsilon_k-\bar{\mu})^2+V_S^2x_S^2}$, $E^{\pm}_{\eta k}=\epsilon_k \pm \sqrt{\bar{\mu}^2+V_\eta^2x_\eta^2}$, $E^{\pm}_{\mathrm{sAF}k}=\bar{\mu}\pm\sqrt{\epsilon_k^2+V_{\mathrm{sAF}}^2x_{\mathrm{sAF}}^2}$, $E^{\pm}_{\mathrm{bAF}k}=\bar{\mu}\pm\sqrt{\epsilon_k^2+V_{\mathrm{bAF}}^2|\eta_k x_{bAF}|^2}$, $E^{\pm}_{\mathrm{sCDW}k}=\bar{\mu}\pm\sqrt{\epsilon_k^2+V_{\mathrm{sCDW}}^2x_{\mathrm{sCDW}}^2}$ and $E^{\pm}_{\mathrm{bCDW}k}=\bar{\mu}\pm\sqrt{\epsilon_k^2+V_{\mathrm{bCDW}}^2|\eta_k x_{\mathrm{bCDW}}|^2}$ for the S, η, sAF, bAF, sCDW, and bCDW phases, respectively. In the derivation of the eigensolutions we have assumed an alternated lattice, i.e., $\epsilon_{k+Q}=-\epsilon_k$.

For arbitrary electron concentration n the stable solutions are determined as the minimum of F with respect to the variational parameters x_α ($\alpha=S,\eta$, sAF, bAF, sCDW, bCDW), p and μ, i.e., by the equations

$$\partial F/\partial x_\alpha = 0,\ \partial F/\partial p = 0,\ \partial F/\partial \mu = 0. \tag{5}$$

Besides the pure phases there are also solutions for various mixed type orderings. We have analyzed the stability conditions for all such states and found that some of them can be stable in a definite range of parameters. They are summarized in Table I together with the corresponding order parameters. For example, we present here the equations describing the mixed s+bAF phase. In this case the free energy (3) is expressed in terms of the eigenstates as

$$\frac{F}{N} = \bar{\mu}(n-1) + \frac{U}{4}n^2 + \frac{4}{z}Jp^2 + V_{sAF}x_{sAF}^2 + 2V_{\mathrm{bAF}}|x_{\mathrm{bAF}}|^2 - \frac{1}{\beta N}\sum_{k,r}\ln\left[2\cosh\left(\frac{\beta E^r_{sbAFk}}{2}\right)\right] \tag{6}$$

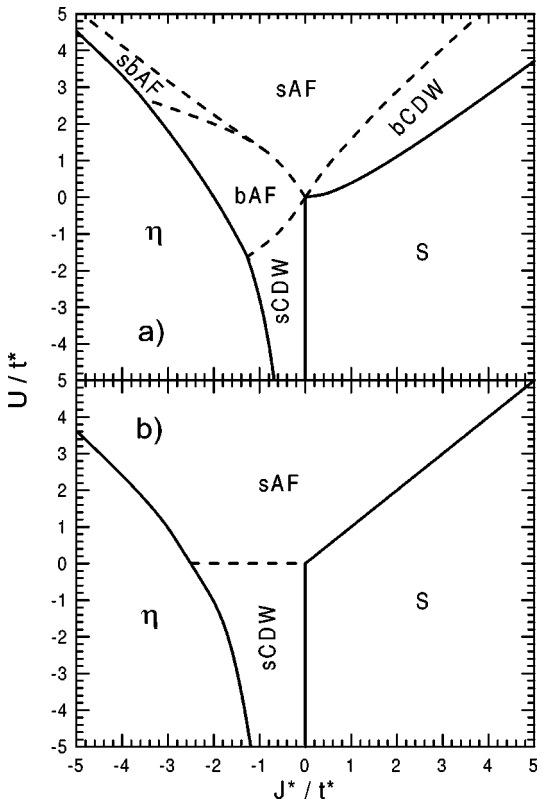

FIG. 1. Phase diagram of the half-filled PKH model for the 1D chain (a) and for the $d=\infty$-hypercubic (b) lattice determined within the broken symmetry HFA. The region of the mixed AF state is denoted by sbAF. Close to the boundary lines separating the sAF and bCDW states as well as the sCDW and bAF states there are very narrow regions (narrower than thickness of the curves in the figure) of the stable mixed ordered phases (sAF+bCDW, for $U>0$ and sCDW+bAF for $U<0$). First-order and second-order transition phase boundaries are marked by solid and dashed curves, respectively. The SBMFA phase diagram for $d=\infty$ is almost identical to (b) (see discussion in Sec. III).

with the electronic spectrum $E^{\pm}_{\mathrm{sbAF}k}=\bar{\mu}\pm\sqrt{\epsilon_k^2+V_{\mathrm{sAF}}^2x_{\mathrm{sAF}}^2+V_{\mathrm{bAF}}^2|\eta_k x_{\mathrm{bAF}}|^2}$ and $x_{\mathrm{sAF}}, x_{\mathrm{bAF}}, p$ and μ are determined by a set of self-consistent equations $\partial F/\partial x_{\mathrm{sAF}}=0, \partial F/\partial x_{\mathrm{bAF}}=0, \partial F/\partial p=0$, and $\partial F/\partial\mu=0$.

In order to determine the mutual stability of the phases considered one has to find all the possible solutions and compare the corresponding free energies. In the weak and strong coupling regimes we were able to derive several analytical expressions concerning the energy gaps, the order parameters, and the critical temperatures, but in a general case numerical methods had to be used. At $T=0$ we performed complete numerical analysis of all the solutions for the whole range of the parameter values and the resulting phase diagrams are presented in Fig. 1 for the 1D chain and the hypercubic lattice of the dimension $d=\infty$. The renormalized parameters are $J^*=Jd$ and $t^*=t\sqrt{d}$.

For $d=\infty$ the density of states (DOS) is $\rho(\epsilon)=\exp[-\epsilon^2/(8t^{*2})]/(\sqrt{8\pi}t^*)$. In this case there are no stable states with the bond type of ordering as all bond parameters disappear in the limit $d\to\infty$. Also, the Fock term p is then irrelevant as the effective width of the electronic band $W_{\mathrm{eff}} \equiv 4\tilde{t}d = 4t^*\sqrt{d} + 4J^*p/d$ and the second term disappears for

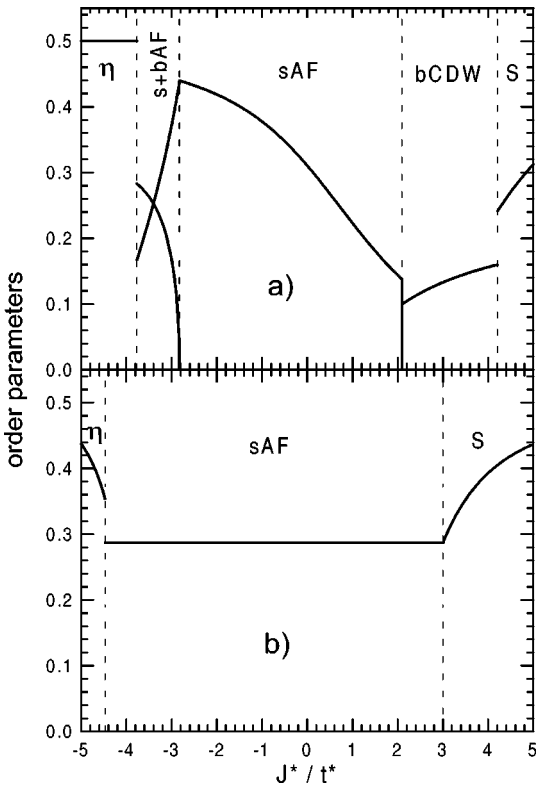

FIG. 2. The J^*/t^* dependence of the order parameters in the ground state of the $d=1$ (a) and $d=\infty$ (b) system, for $n=1$ and $U/t^*=3$. The stability ranges of the different phases are indicated by the vertical dashed lines. The mixed sAF+bCDW state (a) exists for $J^*/t^* \in (2.09105, 2.09425)$.

$d=\infty$. This is in contrast to the $d=1$ case [Fig. 1(a)], where the AF and CDW orderings of the bond type can exist in a wide range of parameters (the former for $J<0$ and the latter for $J>0$). The bond type ordering can also coexist with the on-site type ordering, as it is seen in Fig. 1(a) for the mixed s+bAF phase. There have been also found very narrow regions of the stable mixed phases: bAF+sCDW (for $U<0$) and sAF+bCDW (for $U>0$). The curves separating the sAF- and the bAF-type orderings are the lines of second order phase transition, at which the parameter x_{sAF} or x_{bAF} disappears. In the lattices of dimension $1<d<\infty$ one can analyze more complex bond orderings (e.g., the phase of fluxes), however, the ranges of stability of all the bond-ordered phases will be gradually shrank with increasing lattice dimension.

The J^* dependence of the order parameters for $U/t^*=3$ is presented in Fig. 2, where the upper part is for the $d=1$ system and the lower part for $d=\infty$. Figure 2(a) shows a wide range of the mixed s+bAF phase with $x_{\mathrm{sAF}}\neq 0$ and $x_{\mathrm{bAF}}\neq 0$. The parameter $x_{\mathrm{bAF}}\rightarrow 0$ for $J^*/t^*\rightarrow -2.83$, indicating the second-order transition. In the case presented in Fig. 2(a) ($U/t^*=3$) the mixed sAF+bCDW phase is stable only in a very narrow range $2.09105<J^*/t^*<2.09425$.

III. SLAVE-BOSON STUDIES

In the previous paper[17] we showed that the slave boson mean-field approach (SBMFA) gives reliable results for the ground state properties of the attractive Hubbard model in the whole range of coupling $|U|$ and arbitrary electron concentration n. Therefore, we also applied this method to the present model (1). As the SBMFA takes into account the onsite electron correlations and neglects the short-range intersite correlations (the Fock term and the bond type orderings are omitted), we have concentrated on the case of $d=\infty$ lattice, where the mean field treatment of intersite interactions becomes exact.

In the slave-boson approach each local state is described by a Fermi operator $f_{i\sigma}$ and two types of bose operators $\boldsymbol{p}_i$ and $\boldsymbol{b}_i$, which correspond to two vector fields: a field of local magnetic moments and that of local charges. The completeness condition means that length and direction of the vectors $\boldsymbol{p}_i$ and $\boldsymbol{b}_i$ can vary from site to site, but a sum of their length is always $p_i^2+b_i^2=1$. We use the spin- and the charge-rotationally invariant slave-boson representation,[20,17] in which the order parameters are expressed by $x_S=(1/N)\Sigma_{i,\rho}\langle b_{ix}^\dagger b_{ix}+b_{iy}^\dagger b_{iy}\rangle$, $x_\eta=(1/N)\Sigma_{i,\rho}e^{i\mathbf{QR}_i}\langle b_{ix}^\dagger b_{ix}+b_{iy}^\dagger b_{iy}\rangle$, $x_{\mathrm{sCDW}}=(1/N)\Sigma_i e^{i\mathbf{QR}_i}\langle b_{iz}^\dagger b_{iz}\rangle$, and $x_{\mathrm{sAF}}=(1/N)\Sigma_i e^{i\mathbf{QR}_i}\langle p_{iz}^\dagger p_{iz}\rangle$, for the superconducting sCDW and sAF phases, respectively. In the mean field studies we confine ourselves to the temperature $T=0$ and neglect space and time fluctuations of the bose fields. The operators $\boldsymbol{p}_i$ and $\boldsymbol{b}_i$ are replaced by their expectation values, which in the following are treated as variational parameters. The SBMFA is, therefore, a variational method on a trial state described by the Hartree-Fock wave functions (being equivalent to the Gutzwiller approximation).[21] The free energy is the sum of the fermionic and bosonic parts, and for the α phase, where $\alpha=S,\eta$, sCDW, sAF, and any given n it can be written in the following unified form:

$$\frac{F^{\mathrm{SBMFA}}}{N}=\frac{F_f}{N}+\frac{F_b}{N}$$
$$=-\frac{1}{N\beta}\sum_{k,r}\left[\ln\{1+\exp(\beta E_{\alpha k}^{sbr})\}\right]+\frac{U}{2}(b^2+2\delta)$$
$$+C_\alpha-(\lambda_0+\mu)(1+2\delta)-2\lambda_\alpha x_\alpha, \qquad (7)$$

where $r=\pm$, $C_S=-2J^*x_S^2$, $C_\eta=2J^*x_\eta^2$, $C_{\mathrm{sCDW}}=0$, $C_{\mathrm{sAF}}=0$, $b^2=\langle b_{ix}^\dagger b_{ix}+b_{iy}^\dagger b_{iy}+b_{iz}^\dagger b_{iz}\rangle$, and $2\delta=n-1=\langle b_{iz}^\dagger b_{iz}\rangle$, λ_0 and λ_α are the Lagrange multipliers. The fermionic spectrum is $E_{Sk}^{sb\pm}=\pm\sqrt{(q_S\epsilon_k+\lambda_0)^2+\lambda_S}$, $E_{\eta k}^{sb\pm}=q_\eta\epsilon_k\pm\sqrt{\lambda_0^2+\lambda_\eta^2}$, $E_{\mathrm{sCDW}k}^{sb\pm}=-\lambda_0\pm\sqrt{q_{\mathrm{sCDW}}\epsilon_k^2+\lambda_{\mathrm{sCDW}}^2}$, and $E_{\mathrm{sAF}k}^{sb\pm}=-\lambda_0\pm\sqrt{q_{\mathrm{sAF}}\epsilon_k^2+\lambda_{\mathrm{sAF}}^2}$. Its k dependence is analogous to that obtained in the HFA with the bandwidth reduced by the factor

$$q_\alpha=\frac{2p^2(b^2+\sqrt{b^4-4x_\alpha^2-4\delta^2})}{1-4x_\alpha^2-4\delta^2}, \qquad (8)$$

for $\alpha=S,\eta$, sCDW, and

$$q_{\mathrm{sAF}}=\frac{2b^2(p^2+\sqrt{p^4-4x_{\mathrm{sAF}}^2-4\delta^2})}{1-4x_{\mathrm{sAF}}^2-4\delta^2}. \qquad (9)$$

The stable solutions are determined from the minimum of the free energy F^{SBMFA} with respect to $x_\alpha,\lambda_\alpha,\lambda_0$, and b.

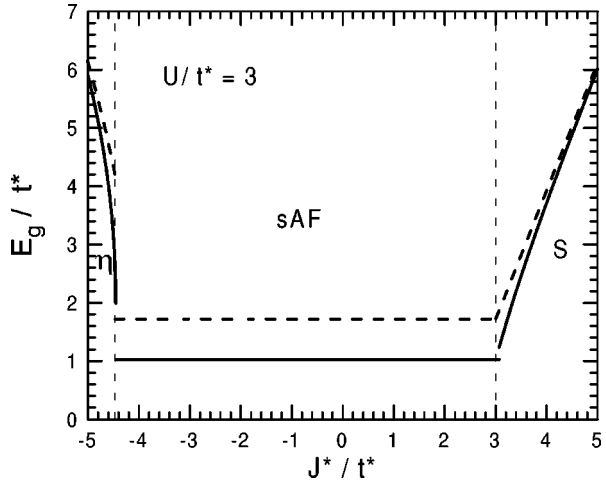

FIG. 3. The dependence of the gap in the excitation spectrum on J^*/t^* calculated in the SBMFA (solid curves) and in the HFA (dashed curves) for $d=\infty$ hypercubic lattice, $U/t^*=3$ and $n=1$. The stability ranges of the different phases are indicated by the vertical dashed lines.

In determination of the phase diagram of the half-filled PKH model we compare the free energies $F_\alpha^{\mathrm{SBMFA}}$ corresponding to the S, η, sCDW, and sAF phases. Their values are different from those obtained in the HFA and depend on the band narrowing factors q_α. These factors are important parameters. In the normal phase ($x_\alpha=0$) the band narrowing process can lead to insulating phase ($q_N=0$) for large coupling $|U|\gg t$.[17,21,20,22] However, for alternating lattices and $n=1$ the normal phase is not a ground state as its free energy is always higher than that of the long-range ordered phases (S, η, sCDW, and sAF). For all these phases the band narrowing factors q_α are close to unity, for example, in the attractive Hubbard model: $0.954<q_S<1$ in $d=\infty$ (see also Ref. 22). Thus, the SBMFA free energies of the ordered phases are relatively close to the corresponding HFA results. The SBMFA phase diagram of the PKH model for $d=\infty$ is, therefore, very similar to that given in Fig. 1(b). In particular, the location of the S-sAF phase boundary in the ground state phase diagram can be expressed most conveniently in terms of the deviation $\epsilon_c=J^*/U-1$ from the line $J^*/U=1$. Within the HFA, the S-sAF phase boundary is given by $J^*/U=1$ for any t^*, and for $d=\infty$ it agrees with a rigorous solution at $t^*=0$.[16] Within the SBMFA, ϵ_c is found to depend sensitively on the strength of the interactions and one obtains that $\epsilon_c>0$ for any $\infty>t^*>0$, with a maximum deviation $\epsilon_c\approx 0.02$ found for $U/t^*\approx 3.5$ and with $\epsilon_c\to 0$ for $t^*\to 0$ as well as $t^*\to\infty$. It means that the hopping term slightly extends the stability range of the sAF phase with respect to the S phase. Notice that similar results are obtained for the extended Hubbard model with nearest neighbor density-density repulsion W^*. In that case Monte Carlo simulations[23] and perturbational treatments[24] show that for $t\neq 0$ the actual phase boundary is also slightly shifted upward relative to the line $W^*/U=1$ predicted by the HFA.

Although the SBMFA gives minor changes in the ground state energies, other physical characteristics are modified in a much more pronounced way. We will show it analyzing the gap E_g in the excitation spectrum determined within the SBMFA as well as the HFA. Figure 3 shows dependences of

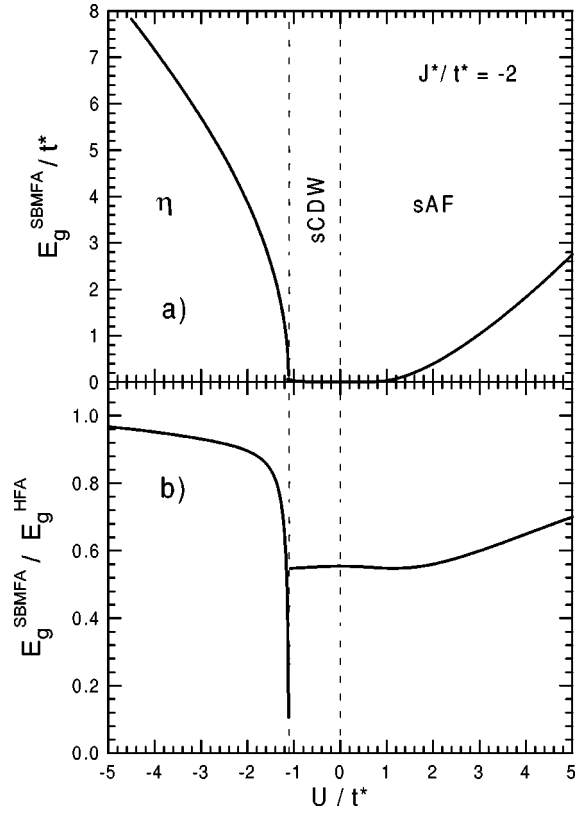

FIG. 4. The plots of the gap in the excitation spectrum (a) and the reduction factor $\gamma_\alpha=E_g^{\mathrm{SBMFA}}/E_g^{\mathrm{HFA}}$ (b) as a function of U/t^*, calculated in the SBMFA for $d=\infty$ hypercubic lattice, $J^*/t^*=-2$ and $n=1$.

E_g on J^* in the case of $U/t^*=3$ and $n=1$. The value of E_g^{SBMFA} is reduced with respect to E_g^{HFA}. The results are closer to each other for larger couplings $|J^*|$, where the onsite correlations become less relevant. The maximum reduction is seen for the gap in the η state, which at the transition line is reduced by a factor $\gamma_\eta\equiv E_{g\eta}^{\mathrm{SBMFA}}/E_{g\eta}^{\mathrm{HFA}}=0.56$. Figure 4 presents the U/t^* dependence of E_g for $J^*/t^*=-2$ and $n=1$. The gaps $E_{g\mathrm{sAF}}$ and $E_{g\mathrm{sCDW}}$ corresponding to the sAF and sCDW phases do not depend on J^*, and they are the same as in the usual Hubbard model ($J^*=0$). In the lower part of Fig. 4 the reduction parameter γ_α is shown. The minimum value of γ_η is 0.11 for $E_{g\eta}^{\mathrm{SBMFA}}$ close to the transition point to the sCDW phase. The energy gaps $E_{g\mathrm{sAF}}^{\mathrm{SBMFA}}$ and $E_{g\mathrm{sCDW}}^{\mathrm{SBMFA}}$ are maximally reduced for a weak coupling $|U/t^*|\ll 1$. In this limit one can find that

$$E_{g\alpha}^{\mathrm{HFA}}=At^*\exp\left[-\frac{\sqrt{8\pi}t^*}{|U|}\right] \tag{10}$$

and

$$\gamma_\alpha\equiv\frac{E_{g\alpha}^{\mathrm{SBMFA}}}{E_{g\alpha}^{\mathrm{HFA}}}=\exp\left[-\frac{3\pi}{16}\right]=0.554855, \tag{11}$$

where $\alpha=$ sAF, sCDW and S, $A=4\sqrt{2}e^{-\gamma/2}=4.23871$, and $\gamma=0.577216$ is the Euler gamma constant. (The value (11) is larger than $\gamma_S=\exp[-3/4]=0.472267$ obtained for the rectangular density of states.[17])

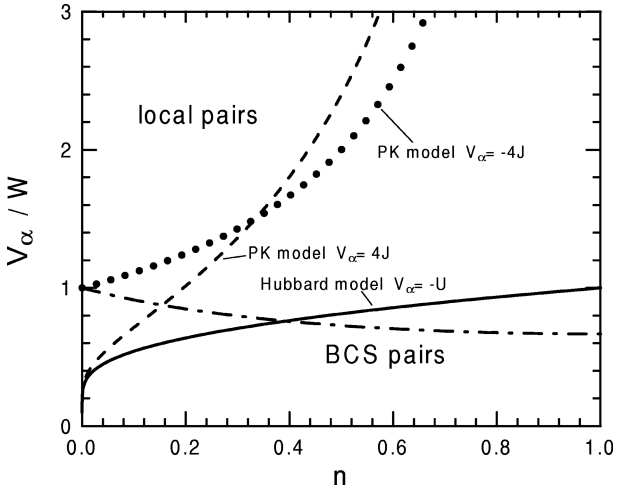

FIG. 5. Boundary lines between the regions of the BCS-like and the local pair superconductivity calculated as a function of n in the case of $d=2$ lattice for the $U<0$ Hubbard model ($V_\alpha=-U$), solid curve, as well as for the PK model with $J>0(V_\alpha=4J,)$ dashed curve, and with $J<0(V_\alpha=-4J)$, dotted curve. For the PK model with $J<0$ the η-type Cooper pairs are stable only above the long-short dashed curve.

IV. DISCUSSION AND CONCLUDING REMARKS

Let us compare the properties of superconducting phases and their evolution with a change of coupling and concentration for the three limiting cases of the model (1): (i) The attractive Hubbard model with $U<0,J=0$, (ii) the PK model with $U=0,J>0$, and (iii) the PK model with $U=0,J<0$. We will discuss qualitative differences and similarities in the behavior of the system for these limits and stress distinct features of each case.

In the first two cases the pairing interaction favors the on-site s-wave superconductivity (S), whereas in the third one, the η pairing. Moreover, the later two cases include a nonlocal pairing mechanism (J) that is distinct from the zero-range instantaneous interaction existing in the (i) case. The difference between (i) and (ii) occurs in the case of the half-filled band. At $n=1$ the $U<0$ Hubbard model posses SU(2) symmetry of the charge sector and is characterized by coexistence of the sCDW and the S ordering (these phases are strictly degenerated) in the ground state. No such degeneracy occurs in the PK model, as its charge sector is governed by the U(1) symmetry for any n.

For (i) and (ii) at $T=0$ the S phase is stable for any nonzero interaction ($U<0$ or $J>0$) and arbitrary n ($0<n<2$). In both these cases the evolution of the S phase from BCS like superconductivity with extended Cooper pairs, to superconductivity of composite bosons (local pairs) with increasing coupling is continuous. At $T=0$ the appropriate boundary between both regimes can be located (after Leggett[25]) from the requirement that the chemical potential in the superconducting phase reaches the bottom of the electronic band, i.e., from $\mu_S=-W/2$. For a $d=2$ lattice the borderlines as a function of n are shown in Fig. 5. As we see for both models with increasing n the boundaries are shifted towards higher values of coupling. For $d=3$ the corresponding plot has qualitatively similar form, except $n\to 0$ limit, where there is a critical value of coupling for pair formation.

For the case (iii) the η phase is stable only below a critical value of J and for $d<\infty$ the local pair regime is reached directly after crossing the η phase boundary. The critical value J_c depends on the lattice structure, the lattice dimensionality (d,) and the band filling (n). The estimations of J_c for various cases are collected in Table II. Except $d=\infty$, the transition at J_c is of the first order and characterized by an abrupt change in the structure of the ground state. For $d=\infty$ the phase stable for $J_c<J<0$ is a normal metal without any long-range ordering (for any n), whereas for $d<\infty$ and $n=1$ that phase is insulating and antiferromagnetic with bond-type modulation of magnetization.

The evolution of the gap parameters $x_\alpha(\alpha=S,\eta,$ and bAF) with increasing interaction V_α (*for all three cases*) is presented in Fig. 6 for $d=1$ [Fig. 6(a)] and $d=\infty$ [Fig. 6(b)]. The corresponding plots for $d=2$ and $d=3$ lattices have qualitatively the same form to those for $d=1$. For the sake of comparison we have shown also the SBMFA results (curves with diamonds in Fig. 6) calculated for the attractive Hubbard model in $d=1$ and $d=\infty$. Notice the first order transition from the bAF state to the η state in the $J<0$ PK model for $d=1$. In this case x_η has the maximum value 1/2. On the contrary for $d=\infty$ the phase transition to the η state is of second order and x_η continuously increases with decreasing J^* (it never saturates for a finite J^*). For the $J>0$ PK model and the $U<0$ Hubbard model one observes a continuous

TABLE II. The HFA estimates of the critical value of J below which the η state has lower energy than the normal state in the PK model with $J<0$. In the limit $n\to 0$ the exact solution is $J_c^*=-W=-2\sqrt{d}t^*$. The results obtained by density matrix renormalization group (Ref. 10) (DMRG), Lanczos diagonalization (Ref. 13), and real space renormalization-group (Ref. 11) (RSRG) methods for the 1D chain are given as well.

System	J_c^*/t^* $n=1$	$n\to 0$ (exact)
$d=1$	$-\pi/2\approx-1.5708$	-2
	-1.5 (Ref. 10) , -1.75 (Ref. 13), -1.65 (Ref. 11)	
$d=2$ square lattice	0	$-2\sqrt{2}\approx-2.8284$
rectangular DOS	$-8/3\sqrt{2}\approx-1.8856$	
$d=3$ sc lattice	-1.7028	$-2\sqrt{3}\approx-3.4641$
elliptic DOS	$-3\sqrt{3}\pi/8\approx-2.0405$	
$d=\infty$	$-\sqrt{2\pi}\approx-2.5066$	$-\infty$

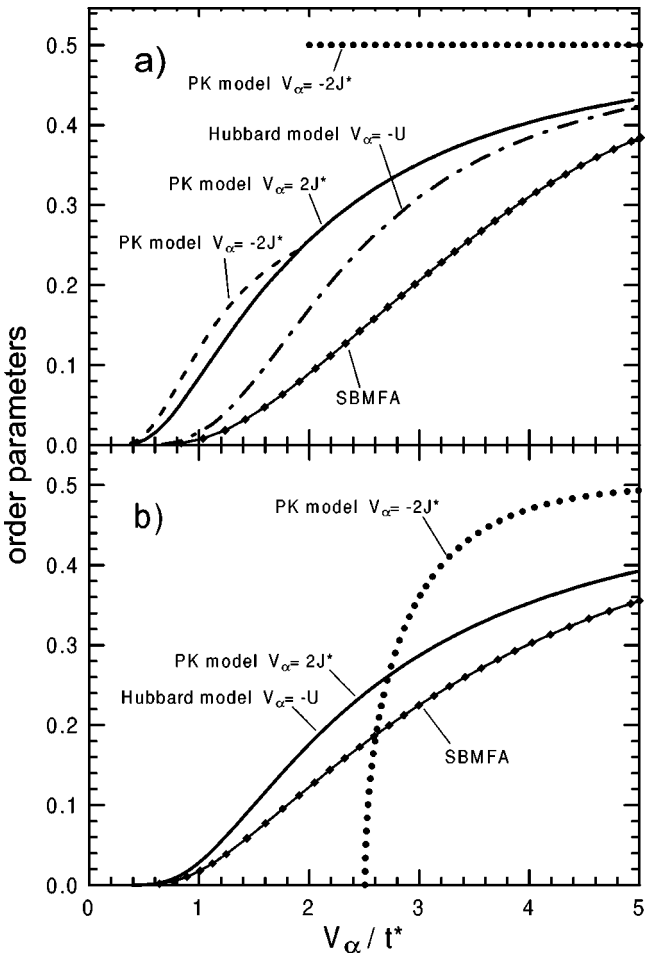

FIG. 6. The plots of the gap parameters $x_\alpha = E_g^\alpha / V_\alpha$ as a function of the coupling parameters V_α for the S phase of the attractive Hubbard model (dashed-dot curve, $V_\alpha = -U$) and the PK model (solid curve, $V_\alpha = 2J^*$) as well as for the η phase (dotted curve) and the bAF phase (dashed curve) of the PK model ($V_\alpha = -2J^*$), calculated within the HFA, in the case of $d=1$ (a) and $d=\infty$ (b) lattices, $n=1$. For $d=\infty$ the plots of x_S vs V_α for the PK model and the $U<0$ model have the same form (solid curve). For the sake of comparison the SBMFA results for the $U<0$ Hubbard model in $d=1$ and $d=\infty$ are presented by the curves with diamonds.

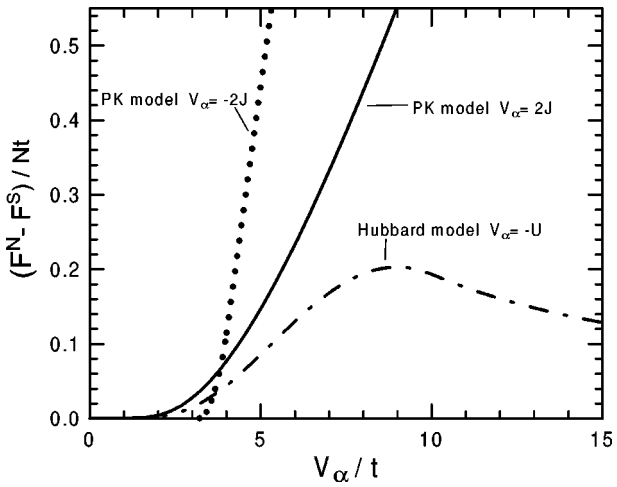

FIG. 7. Difference between the free energies for the normal and the superconducting phase plotted as a function of coupling parameters V_α for the attractive Hubbard model (dashed-dot curve, $V_\alpha = -U$) and the PK model (solid curve, $V_\alpha = 2J$) as well as the difference of the free energies for the normal and the η-type superconducting phase for the PK model vs $V_\alpha = -2J$ (dotted curve). The derivations were performed for the $d=1$ chain at $n=0.8$ and $T=0$ by means of the SBMFA for the attractive Hubbard model and by the HFA for the PK model.

evolution of the order parameter x_S with increasing V_α and an exponential (BCS-like) behavior of x_S in the weak coupling limit.

As we have already pointed out, for both models there is a crossover from the BCS-like limit to the tightly bound pairs regime with increasing coupling and this evolution of the superconducting (S) phase is gradual. However, the thermodynamic and electromagnetic properties of both the models are very different beyond the weak coupling limit.[17,26] To illustrate the situation we have plotted in Fig. 7 the condensation energies, i.e., the difference of the free energy in the normal and in the superconducting phase, $\Delta F = F^N - F^S$, as a function of the coupling parameters V_α. These results have been obtained for the $d=1$ chain at $n=0.8$, but for the lattices of other dimension and other electron concentrations one gets qualitatively similar dependences. They are in good qualitative agreement with results of perturbational expansions for the models considered both in the weak coupling ($V_\alpha/t \ll 1$) as well as in the strong coupling regimes ($V_\alpha/t \gg 1$).[17,26] As the square of the thermodynamic critical field H_c^2 is proportional to ΔF, we conclude that in the attractive Hubbard model this quantity (similarly as the critical temperature T_c) increases exponentially for small values of $|U|$, then goes through a round maximum and decreases as $t^2/|U|$ for large $|U|$. On the contrary, in the PK model we found no maximum of H_c^2 and T_c at intermediate coupling and both these quantities increase linearly with J for large J. Also the behavior of the penetration depth λ_L and the pair mobility t_p is different. In the strong coupling limit $\lambda_L^2 \propto 1/t_p$ *increases* with $|U|$ in the former model ($\lambda_L^2 \propto |U|/t^2$), while it *decreases* with J in the PK model ($\lambda_L^2 \propto 1/J$). It is in agreement with studies of collective excitations performed using a generalized random-phase approximation.[14] The collective-mode velocity increases with J in the PK model, in contrast to the attractive Hubbard model where it decreases with the coupling $|U|$.

The phase diagram of the half-filled one-dimensional PK model ($U=0, J\neq 0$) derived within the HFA is in agreement with that obtained by the density matrix renormalization group method.[7,10,12] For $J>0$ both approaches predict a continuous second-order transition to usual s-wave pairing state at $J=0^+$, with no additional transition for any $J>0$ (in contrast to the earlier predictions[8,11]). We have found that (at least for alternating lattices) this phenomenon remains unchanged in higher dimensions (including the exactly solvable case of $d=\infty$) and does not depend on the band filling. With increasing coupling there is a gradual crossover from the BCS-like superconductivity to the superfluidity of tightly bound local pairs. On the contrary, for $J<0$ the HFA predicts that the η phase is stable only above a critical value of $|J|$ and that the transition at J_c is of the first order for any $d<\infty$. Let us stress that for $n=1$ the values of J_c calculated within the HFA are in very good quantitative agreement with

the results of other more elaborated treatments available for the $d=1$ chain[10,11,13] (see Table II). Moreover for $n\to 0$ the HFA yields exact results for J_c for any dimension.

We have found that the interplay between the on-site Coulomb interaction U and the intersite pair hopping J in the PKH model can stabilize several new ordered phases absent in the usual Hubbard model ($U\neq 0, J=0$) and in the usual PK model ($U=0, J\neq 0$): the bCDW and the mixed bCDW +sAF phases (for $U>0, J>0$), the mixed s+bAF phase (for $U>0, J<0$), as well as the sCDW and the mixed bAF +sCDW phases (for $U<0, J<0$). The new phases predicted by our broken symmetry HFA approach (which can be truly long range in $d\geqslant 2$) indeed need further examination by more rigorous methods such as the exact diagonalization of small systems, density renormalization group, etc. We should point out, however, that our findings concerning the bond-ordered solutions are clearly supported by recent work of Japaridze and Müller-Hartmann[15] performed for the $d=1$ PKH model with $U\geqslant 0$ in weak coupling, using the continuum limit field theory approach and bosonization technique. In contrast to previous studies,[8,9,11] which have not considered the possibility of bond-located orderings, present results and those of Ref. 15 indicate that the bCDW (bAF) state but not the sAF or sCDW phases, is unstable with respect to transition into the S (η) phase with increasing J ($-J$) for $U>0$.

We have also compared the superconducting properties of the PK model with those of the attractive Hubbard model. Although the energy gaps have similar dependences on the coupling parameters in the both models (see also Ref. 12), dynamics of electron pairs is qualitatively different, which results in different electrodynamic properties and different coupling dependences of T_c, especially in a strong coupling regime.

ACKNOWLEDGMENTS

The paper was supported from the State Committee for Scientific Research Republic of Poland within Grant No. 2 P03B 104 11 (S.R.) and 2 P03B 075 14 (B.R.B). We wish to thank R. Micnas for useful comments and discussions.

*Electronic address: saro@phys.amu.edu.pl
†Electronic address: bulka@ifmpan.poznan.pl

[1] K. A. Penson and M. Kolb, Phys. Rev. B **33**, 1663 (1986); J. Stat. Phys. **44**, 129 (1986).
[2] R. Micnas, J. Ranninger, and S. Robaszkiewicz, Rev. Mod. Phys. **62**, 113 (1990).
[3] J. Hubbard, Proc. R. Soc. London, Ser. A **276**, 238 (1963); D. K. Campbell, J. T. Gammel and E. Y. Loh, Phys. Rev. B **42**, 475 (1990); J. E. Hirsch, Physica C **179**, 317 (1991); J. C. Amadon and J. E. Hirsch, *ibid.* **54**, 6464 (1996).
[4] E. Fradkin and J. E. Hirsch, Phys. Rev. B **27**, 1680 (1983); K. Miyake, T. Matsuura, H. Jichu, and Y. Nagaoka, Prog. Theor. Phys. **72**, 1063 (1983).
[5] S. Robaszkiewicz, R. Micnas, and J. Ranninger, Phys. Rev. B **36**, 180 (1987).
[6] C. Bastide and C. Lacroix, J. Phys. C **21**, 3557 (1988).
[7] I. Affleck and J. B. Marston, J. Phys. C **21**, 2511 (1988).
[8] A. Hui and S. Doniach, Phys. Rev. B **48**, 2063 (1993).
[9] A. Belkasri and F. D. Buzatu, Phys. Rev. B **53**, 7171 (1996).
[10] A. E. Sikkema and I. Affleck, Phys. Rev. B **52**, 10 207 (1995).
[11] B. Bhattacharyya and G. K. Roy, J. Phys.: Condens. Matter **7**, 5537 (1995).
[12] M. van den Bossche and M. Caffarel, Phys. Rev. B **54**, 17 414 (1996).
[13] G. Bouzerar and G. I. Japaridze, Z. Phys. B **104**, 215 (1997).
[14] G. K. Roy and B. Bhattacharyya, Phys. Rev. B **55**, 15 506 (1997).
[15] G. I. Japaridze and E. Müller-Hartmann, J. Phys.: Condens. Matter **9**, 10 509 (1997).
[16] S. Robaszkiewicz and G. Pawłowski, Physica C **210**, 61 (1993); S. Robaszkiewicz, Acta Phys. Pol. A **85**, 117 (1994).
[17] B. R. Bułka and S. Robaszkiewicz, Phys. Rev. B **54**, 13 138 (1996).
[18] Obviously, in more general cases (i.e., for nonalternating lattices or longer-ranged hoppings t_{ij} as well as $n\neq 1$) the number of possible ordered states can be much larger, including also various types of incommensurate phases, phase of vortices, phase-separated states, etc. We postpone discussion of this subject to a forthcoming paper.
[19] S. V. Tyablikov, *Methods in the Quantum Theory of Magnetism* (Plenum, New York, 1967).
[20] R. Frésard and P. Wölfle, Int. J. Mod. Phys. B **6**, 685 (1992).
[21] G. Kotliar and A. E. Ruckenstein, Phys. Rev. Lett. **57**, 1362 (1986).
[22] M. Bak and R. Micnas, Mol. Phys. Rep. **20**, 91 (1996); J. Phys.: Condens. Matter **10**, 9029 (1998).
[23] J. E. Hirsch, Phys. Rev. Lett. **53**, 2327 (1984).
[24] A. M. Oleś, R. Micnas, S. Robaszkiewicz, and K. A. Chao, Phys. Lett. **102A**, 323 (1984); P. G. J. van Dongen, Phys. Rev. B **49**, 7904 (1994).
[25] A. J. Leggett, in *Modern Trends in the Theory of Condensed Matter*, edited by A. Pekalski and J. Przystawa (Springer-Verlag, Berlin, 1980), p. 13.
[26] S. Robaszkiewicz and B.R. Bułka (unpublished).